

Communication

Fluorescence and Naked-Eye Detection of Pb^{2+} in Drinking Water Using a Low-Cost Ionophore Based Sensing Scheme

Aron Hakonen ^{1,2,*}  and Niklas Strömberg ² 

¹ Sensor Visions AB, Legendgatan 116, SE-422 55 Hisings Backa, Sweden

² RISE Research Institutes of Sweden, Box 857, SE-50115 Borås, Sweden; niklas.stromberg@ri.se

* Correspondence: hakonen@chalmers.se; Tel.: +46-708-411-417

Received: 7 October 2018; Accepted: 6 November 2018; Published: 8 November 2018



Abstract: Drinking water contamination of lead from various environmental sources, leaching consumer products, and intrinsic water-pipe infrastructure is still today a matter of great concern. Therefore, new highly sensitive and convenient Pb^{2+} measurement schemes are necessary, especially for in-situ measurements at a low cost. Within this work dye/ionophore/ Pb^{2+} co-extraction and effective water phase de-colorization was utilized for highly sensitive lead measurements and sub-ppb naked-eye detection. A low-cost ionophore Benzo-18-Crown-6-ether was used, and a simple test-tube mix and separate procedure was developed. Instrumental detection limits were in the low ppt region (LOD = 3, LOQ = 10), and naked-eye detection was 500 ppt. Note, however, that this sensing scheme still has improvement potential as concentrations of fluorophore and ionophore were not optimized. Artificial tap-water samples, leached by a standardized method, demonstrated drinking water application. Implications for this method are convenient in-situ lead ion measurements.

Keywords: lead ions; fluorescence detection; ionophore; Benzo-18-Crown-6-ether; drinking water

1. Introduction

Environmental lead contamination in water, food, and consumer products are still alarming problems [1–7]. Therefore, new highly sensitive and selective lead measurements are necessary, in particular for convenient field measurements at a low-cost [1–5,8]. Currently common and reliable detection methods for lead ions in drinking water and many other products mostly depend on laboratory analysis with instruments such as ICP-OES or ICP-MS or graphite furnace atomic absorption spectroscopy, which are by no means simple, cheap, or portable [2,9]. A recurrent reason for lead contaminated drinking water within cities is ageing water supply infrastructure such as in the Flint water crisis [10], which also revealed dangers regarding lead exposure, especially for children [10]. The US Environmental Protection Agency (EPA) says that 10–20% of US residents' exposure to lead comes from contaminated water and babies can even get up to 60% of their exposure to lead by drinking formula mixed with contaminated water. EPAs permissible limit of lead in drinking water is 15 ppb [11], while The World Health Organization (WHO) recommendation is even lower at 10 ppb [12].

Within this work dye/ionophore/ Pb^{2+} co-extraction and effective water phase de-colorization, and consequent fluorescence decline, is utilized for highly sensitive lead measurements and sub-ppb naked-eye detection. A simple test-tube mix, shake and separate procedure was developed. Prize per sample is extremely competitive and without any cost-optimization the total cost for the chemicals for one sample is ~0.1 US\$. Miniaturized instrumentation for high-performance field measurements can be built for less than 50 UD\$. Generality and easy ionophore replacement is not claimed here and the opposite is actually demonstrated with another more common (and 100-times more expensive) lead

ionophore. Though, carefully considered (of the whole system) most ionophores should be possible utilize in a similar way. A real life sample, a “lead-free” manometer for a coffee machine, was tested according to a standardized leaching test protocol and cross-correlated with ICP-OES with good results. Lead contamination is especially challenging in for example coffee machines, due to the long-term heating of water and consequent accelerated leaching of lead and other species.

2. Materials and Methods

2.1. Instruments

The fluorescence experiments were performed on a FluoroMax 4 spectrofluorometer from: Jobin Yvon (Horiba Group Inc., Kyoto, Japan). Excitation and emission matrix spectra were collected with slit widths corresponding to 2 nm bandpass; integration times were set to 0.1 s and 10 nm steps were used.

2.2. Chemicals

1-Octanol, Merocyanine 540 (90%) and Benzo-18-Crown-6-ether (98%) were all reagent grade and purchased from Sigma-Aldrich (Saint Louis, MO, USA). MilliQ water (electric resistivity $> 18 \text{ M}\Omega\text{cm}^{-1}$) was obtained from a Millipore water purification system. For standards 1000 mg/L Pb, ($\text{Pb}(\text{NO}_3)_2$ in H_2O) Titrisol[®] (109969) was used and diluted with MilliQ water.

2.3. Experimental

2 mL octanol (with Benzo-18-Crown-6-ether 0.5 mg/mL), 1 mL Merocyanine 540 (15 μM in MilliQ water) and 1 mL water sample is mixed thoroughly in a 5 mL glass test-tube, which gave a pink opaque solution (emulsion), that was allowed to separate for 15 min. After which naked-eye and/or fluorescence measurements were performed directly in the test-tube lower water phase.

3. Results

The research conducted here was initiated with attempted developments of a previously published nanoparticle enhanced ammonium and ammonia optical sensor [13–15]. The intention was to expand the portfolio for ionophore/coextraction based optical chemosensors with lead sensors. Several lead ionophores were tested without success, both with and without plasmonic nanoparticles. Therefore, the principles used and developed here were initially performed to understand the sensing mechanism at a macroscopic level in a test tube.

Figure 1 shows test-tubes with separated solutions with zero and 500 ppm lead ions. Also, the proposed sensing mechanism is illustrated in Figure 1, where the Benzo-18-Crown-6-ether collects Pb^{2+} ions and ion pairs with two Merocyanine 540 (one negative charge each) molecules and co-extracts into the less polar octanol phase, with consequent de-colorization and fluorescence decrease in the water phase. Resulting excitation/emission fluorescence matrices are shown in Figure 2A–D for 0/10/500 ppt and 500 ppm lead ions, and a declining fluorescence trend is realized. Another Pb^{2+} ionophore (Lead IV, Selectophore) was tested in the same way with much lower responses. Naked eye detection of 500 ppt lead ions was assessed with both ionophores and pictures are shown in Figure 3A, with an advantage for Benzo-18-Crown-6-ether. This is an indication that all ionophores will not perform on this high level by default in this set-up.

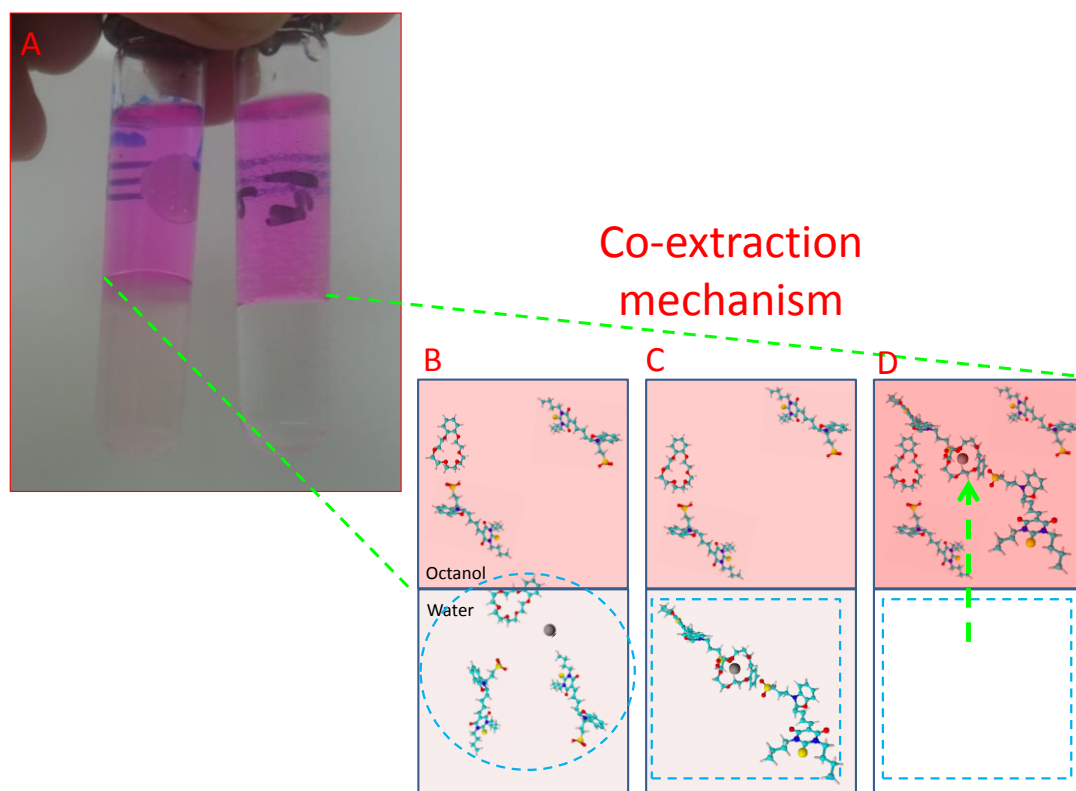


Figure 1. (A) test tubes with separated octanol/water sensor cocktails: zero level (left) and 500 ppm Pb^{2+} . (B) Cartoon showing the co-extraction three step principle by (B) Pb^{2+} introduction near one Benzo-18-Crown-6-ether and two Merocyanine 540 molecules. (C) Complexation; (D) phase transfer.

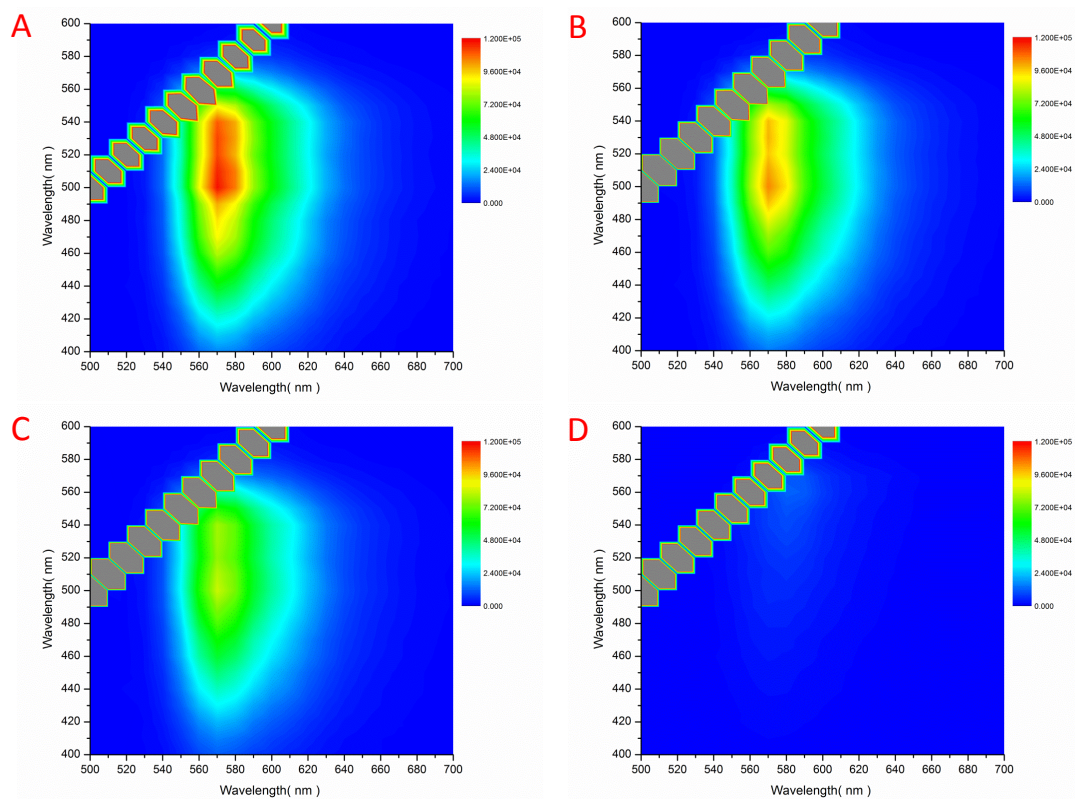


Figure 2. Fluorescence excitation/emission matrix scans of the water phase for Pb^{2+} ion concentrations of: (A) 0 (B) 10 ppt (C) 500 ppt (D) 500 ppm. Note that the intensity scales are set the same.

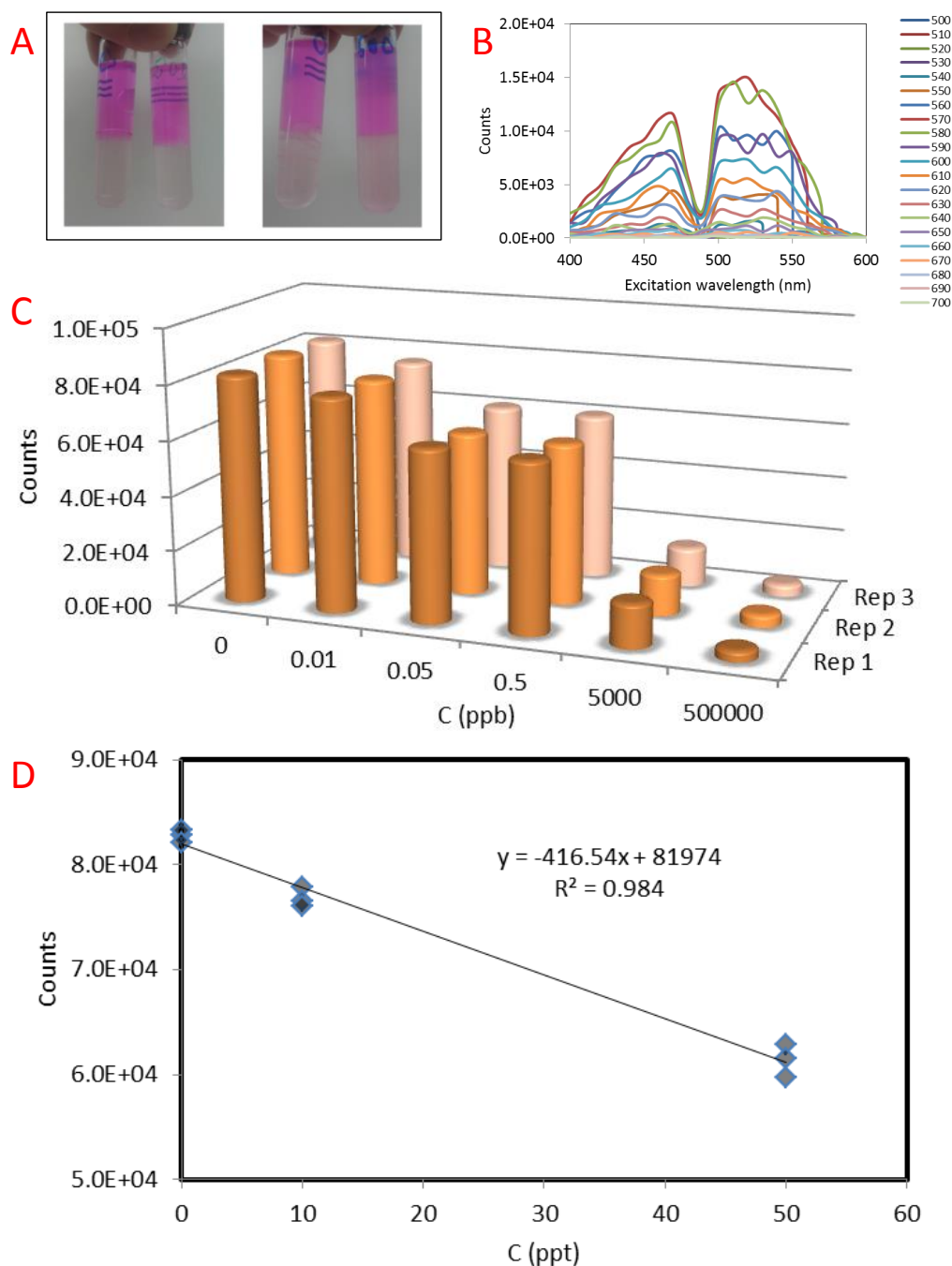


Figure 3. (A) Naked eye detection of 500 ppt Pb²⁺ (left tube), and with less sensitive Lead IV ionophore (right) as comparison. (B) Finding optimized fluorescence wavelengths. (C) Repeatability at different concentrations, first repetition on each concentration in dark orange, second in medium orange and third in light orange. (D) Low ppt level calibration curve for the optimized Ex480/Em580 wavelengths. Limits of detection (LOD) = 3 ppt LOQ = 10 ppt.

To find maximum signal responses difference excitation spectra for zero—10 ppt was calculated (Figure 3B). Ex520/Em570 nm showed maximum response. However, often this may not be the same as best signal to noise ratio, which can be found by dividing the signal by zero level standard deviation [16,17]. Here, optimum S/N ratio \rightarrow $S/N = 9.8$ was found for 10 ppt response at Ex480/Em580 nm, which also demonstrated a high signal in Figure 3B. The repeatability of this wavelength pair at different concentrations are shown in Figure 3C. To calculate limits of detection (LOD) and quantification (LOQ) a calibration curve for the low ppt range was constructed (Figure 3D).

The response at 0–50 ppt was linear with a good correlation coefficient ($R^2 = 0.984$) and excellent detection limits were calculated (LOD = 3 ppt and LOQ = 10 ppt). A real sample: a coffee machine manometer was leached according to the requirements in SS-EN 16889:2016. The quantity of migrated lead in the test water shall not exceed the guideline value of 0.01 mg/kg (10 ppb). The leached manometer ICP-OES result was 3.5 ± 0.7 ppb, while the fluorescence method result was 3.0 ± 0.04 ppb, i.e., in good correlation.

A (or the) major interference Cu^{2+} was experimentally tested and compared with Pb^{2+} with regards to fluorescence response with the Benzo-18-Crown-6-ether as ionophore. The result of this is shown in Figure 4.

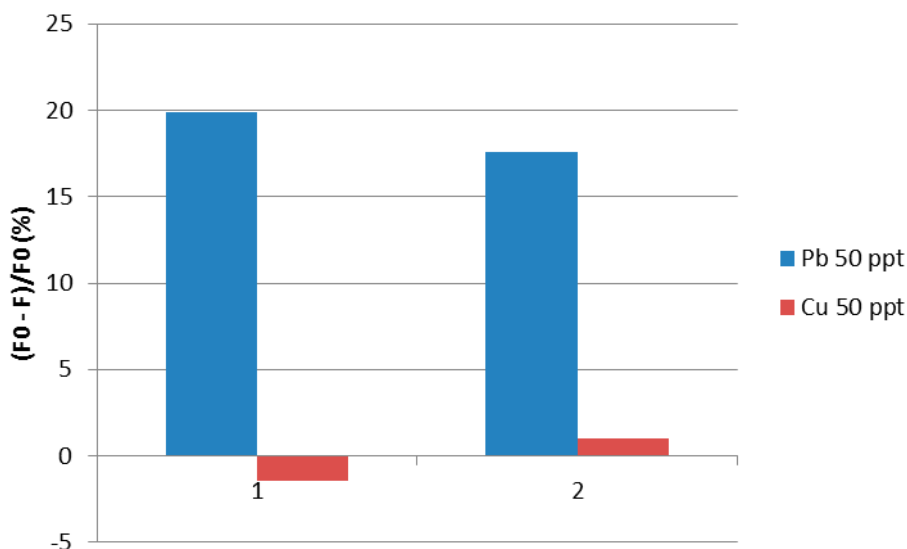


Figure 4. Relative fluorescence signal response for duplicate samples of 50 ppt Pb^{2+} (blue) and Cu^{2+} (red), respectively. Benzo-18-Crown-6-ether was used as ionophore for both ions.

4. Discussion

With regards to selectivity the Benzo-18-Crown-6-ether has been demonstrated as highly selective over its five major interferences and demonstrated an average selectivity coefficient for those of $\text{pK}_{5A} = 5.34$ (Ion:pK; Ca^{2+} :5.2; Mg^{2+} :6.3; Cu^{2+} :4.7; Zn^{2+} : 4.9; Cd^{2+} :5.6), which was almost as good as the more commonly used Lead IV ionophore (Selectophore™) [18,19]. This was also the main reason to involve Benzo-18-Crown-6-ether within this study. The detection method is different, but the complexation and co-extraction take place similarly, hence, similar selectivity is expected. A brief selectivity test towards sodium ions was conducted and demonstrated that 1 ppm Na^+ gave the same response as 100 ppt Pb^{2+} ions indicating 10,000 or 5 orders of magnitude in signal response increase (i.e., similar to the $\text{pK}_{5A} = 5.34$ mentioned above) [19]. For the major interference Cu^{2+} low level detection (50 ppt) was compared (Figure 4), with 18–20% relative signal response for Pb^{2+} and –1–1% for Cu^{2+} .

Comparisons and a brief overview of literature shows that laboratory instrumental techniques for lead measurements commonly involve ICP-MS (LOD low ppt range) and ICP-OES (LOD low ppb range) [20]. Among potential ultra-sensitive in-situ sensing/detection techniques for drinking water one of the better competitors demonstrate a naked-eye detection of 2 ppb and an instrumental semi-quantitative detection of 190 ppt (0.19 ng/mL) [9]. Further, a recent article demonstrated an interesting lab in syringe concept for in-situ detection of lead ions with a LOD = 23 nmol L^{-1} (5 ppb) [5]. Another technique, a label-free impedimetric sensing system based on DNAzyme and ordered mesoporous carbon–gold nanoparticles, showed a LOD of 0.2 nmol L^{-1} (40 ppt) [21]. Another DNAzyme based detection scheme demonstrated a detection limit of 0.7 nM (130 ppt) [22]. One among the top-notch fluorescence techniques for Pb^{2+} ions demonstrated a detection limit of

1 nmol L⁻¹ (200 ppt), using a polyguanine (G(33))/terbium ions (Tb(3+)) conjugate [23]. The best fluorescence detection we found to date are another DNAzyme technique showing a detection limit of 0.06 nmol L⁻¹ (12 ppt) [24]. Additionally, there are convenient commercial colorimetric test sticks for Pb²⁺ detection, for example MQuant™ from Merck. However, these test sticks are restricted by a detection limit on the order of low ppm levels.

5. Conclusions

Ultra-sensitive fluorescence and naked-eye detection of Pb²⁺ in drinking water was demonstrated using low-cost Benzo-18-Crown-6-ether as selection ionophore. A simple test-tube mix and separate technique was successfully developed. Instrumental detection limits were in the low ppt region (LOD = 3, LOQ = 10), and naked-eye detection was on the order of 500 ppt. Coffee machine water samples, leached by a standardized method, correlated well with ICP-OES. Implications are simple and ultra-sensitive lead ion measurements in the field.

Author Contributions: Within this study the author contributions were: conceptualization, A.H. and N.S.; methodology, A.H. and N.S.; validation, A.H. and N.S.; formal analysis, A.H.; investigation, A.H. and N.S.; writing—original draft preparation, A.H.; writing—review and editing, A.H. and N.S.; visualization, A.H. and N.S.

Conflicts of Interest: The authors declare no conflict of interest.

References

1. Maity, A.; Sui, X.; Tarman, C.R.; Pu, H.; Chang, J.; Zhou, G.; Ren, R.; Mao, S.; Chen, J. Pulse-Driven Capacitive Lead Ion Detection with Reduced Graphene Oxide Field-Effect Transistor Integrated with an Analyzing Device for Rapid Water Quality Monitoring. *ACS Sens.* **2017**, *2*, 1653–1661. [CrossRef] [PubMed]
2. Batista, É.F.; Augusto, A.D.S.; Pereira-Filho, E.R. Chemometric evaluation of Cd, Co, Cr, Cu, Ni (inductively coupled plasma optical emission spectrometry) and Pb (graphite furnace atomic absorption spectrometry) concentrations in lipstick samples intended to be used by adults and children. *Talanta* **2016**, *150*, 206–212. [CrossRef] [PubMed]
3. Ratnarathorn, N.; Chailapakul, O.; Dungchai, W. Highly sensitive colorimetric detection of lead using maleic acid functionalized gold nanoparticles. *Talanta* **2015**, *132*, 613–618. [CrossRef] [PubMed]
4. Martín-Yerga, D.; Álvarez-Martos, I.; Blanco-López, M.C.; Henry, C.S.; Fernández-Abedul, M.T. Point-of-need simultaneous electrochemical detection of lead and cadmium using low-cost stencil-printed transparency electrodes. *Anal. Chim. Acta* **2017**, *981*, 24–33. [CrossRef] [PubMed]
5. Šrámková, I.H.; Horstkotte, B.; Fikarová, K.; Sklenářová, H.; Solich, P. Direct-immersion single-drop microextraction and in-drop stirring microextraction for the determination of nanomolar concentrations of lead using automated Lab-In-Syringe technique. *Talanta* **2018**, *184*, 162–172. [CrossRef] [PubMed]
6. Ding, S.; Ali, A.; Jamal, R.; Xiang, L.; Zhong, Z.; Abdiryim, T.; Ding, S.; Ali, A.; Jamal, R.; Xiang, L.; et al. An Electrochemical Sensor of Poly(EDOT-pyridine-EDOT)/Graphitic Carbon Nitride Composite for Simultaneous Detection of Cd²⁺ and Pb²⁺. *Materials* **2018**, *11*, 702. [CrossRef] [PubMed]
7. Dai, Y.; Liu, C.; Dai, Y.; Liu, C.C. A Simple, Cost-Effective Sensor for Detecting Lead Ions in Water Using Under-Potential Deposited Bismuth Sub-Layer with Differential Pulse Voltammetry (DPV). *Sensors* **2017**, *17*, 950. [CrossRef]
8. Finšgar, M.; Majer, D.; Maver, U.; Maver, T. Reusability of SPE and Sb-Mmodified SPE Sensors for Trace Pb(II) Determination. *Preprints* **2018**. [CrossRef]
9. Kuang, H.; Xing, C.; Hao, C.; Liu, L.; Wang, L.; Xu, C. Rapid and highly sensitive detection of lead ions in drinking water based on a strip immunosensor. *Sensors* **2013**, *13*, 4214–4224. [CrossRef] [PubMed]
10. Hanna-Attisha, M.; LaChance, J.; Sadler, R.C.; Schnepf, A.C. Elevated Blood Lead Levels in Children Associated With the Flint Drinking Water Crisis: A Spatial Analysis of Risk and Public Health Response. *Am. J. Public Health* **2016**, *106*, 283–290. [CrossRef] [PubMed]
11. United States Environmental Protection Agency (EPA). Lead and Copper Rule. Available online: <https://www.epa.gov/dwreginfo/lead-and-copper-rule> (accessed on 26 May 2018).

12. Lead in Drinking-Water Background Document for Development of WHO Guidelines for Drinking-Water Quality. Available online: http://www.who.int/water_sanitation_health/dwq/chemicals/lead.pdf (accessed on 26 May 2018).
13. Hakonen, A.; Strömberg, N. Diffusion consistent calibrations for improved chemical imaging using nanoparticle enhanced optical sensors. *Analyst* **2012**, *137*. [[CrossRef](#)] [[PubMed](#)]
14. Strömberg, N.; Hakonen, A. Plasmon enhanced imaging of ammonia release from biological tissues using optodes. *Anal. Chim. Acta* **2011**, *704*. [[CrossRef](#)] [[PubMed](#)]
15. Hakonen, A.; Strömberg, N. Plasmonic nanoparticle interactions for high-performance imaging fluorosensors. *Chem. Commun.* **2011**, *47*. [[CrossRef](#)] [[PubMed](#)]
16. Hakonen, A. Plasmon enhancement and surface wave quenching for phase ratiometry in coextraction-based fluorosensors. *Anal. Chem.* **2009**, *81*. [[CrossRef](#)] [[PubMed](#)]
17. Hakonen, A. Fluorescence ratiometric properties induced by nanoparticle plasmonics and nanoscale dye dynamics. *Sci. World J.* **2013**, *2013*. [[CrossRef](#)] [[PubMed](#)]
18. Parra, E.J.; Blondeau, P.; Crespo, G.A.; Rius, F.X. An effective nanostructured assembly for ion-selective electrodes. An ionophore covalently linked to carbon nanotubes for Pb²⁺ determination. *Chem. Commun.* **2011**, *47*, 2438–2440. [[CrossRef](#)] [[PubMed](#)]
19. Sun, L.; Sun, C.; Sun, X. Screening highly selective ionophores for heavy metal ion-selective electrodes and potentiometric sensors. *Electrochim. Acta* **2016**, *220*, 690–698. [[CrossRef](#)]
20. Skoog, D.A.; Holler, F.J.; Crouch, S.R. *Principles of Instrumental Analysis*; Cengage Learning, Inc.: Mason, OH, USA, 2017.
21. Zhou, Y.; Tang, L.; Zeng, G.; Zhang, C.; Xie, X.; Liu, Y.; Wang, J.; Tang, J.; Zhang, Y.; Deng, Y. Label free detection of lead using impedimetric sensor based on ordered mesoporous carbon–gold nanoparticles and DNAzyme catalytic beacons. *Talanta* **2016**, *146*, 641–647. [[CrossRef](#)] [[PubMed](#)]
22. Zhu, Y.; Deng, D.; Xu, L.; Zhu, Y.; Wang, L.; Qi, B.; Xu, C. Ultrasensitive detection of lead ions based on a DNA-labelled DNAzyme sensor. *Anal. Methods* **2015**, *7*, 662–666. [[CrossRef](#)]
23. Lin, Y.-W.; Liu, C.-W.; Chang, H.-T. Fluorescence detection of mercury(II) and lead(II) ions using aptamer/reporter conjugates. *Talanta* **2011**, *84*, 324–329. [[CrossRef](#)] [[PubMed](#)]
24. Wen, Y.; Wang, L.; Li, L.; Xu, L.; Liu, G.; Wen, Y.; Wang, L.; Li, L.; Xu, L.; Liu, G. A Sensitive and Label-Free Pb(II) Fluorescence Sensor Based on a DNAzyme Controlled G-Quadruplex/Thioflavin T Conformation. *Sensors* **2016**, *16*, 2155. [[CrossRef](#)] [[PubMed](#)]



© 2018 by the authors. Licensee MDPI, Basel, Switzerland. This article is an open access article distributed under the terms and conditions of the Creative Commons Attribution (CC BY) license (<http://creativecommons.org/licenses/by/4.0/>).